

Supplemental materials for
**Reconstructing molecular orbitals with laser-induced
electron tunneling spectroscopy**

XuanYang Lai, RenPing Sun, ShaoGang Yu, YanLan Wang, Wei Quan, André Staudte, XiaoJun Liu

1. Experimental setup

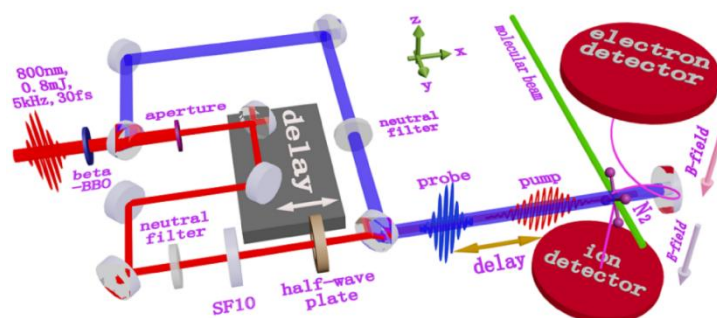


Fig. S1: Experimental setup. An 800 nm, 0.8 mJ, 5 kHz, 30 fs laser pulse is frequency doubled by a -BBO crystal. The two-color laser fields are then split into an 800 nm alignment pulse and a 400 nm probe pulse. The two pulses are focused into a supersonically cooled gas jet of molecule N_2 in the apparatus of COLTRIMS. The probe pulse, which is applied after a time delay, ionizes the molecules aligned by the alignment pulse.

2. Measured photoelectron energy spectra of N_2

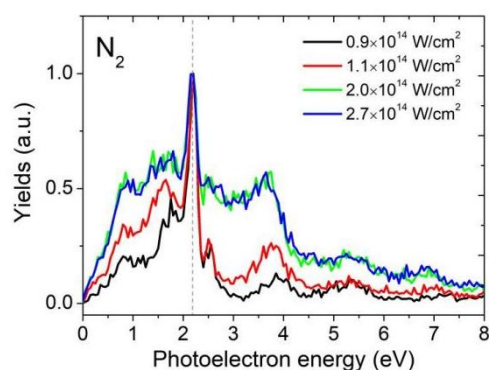


Fig. S2: Measured photoelectron energy spectra of N_2 in the strong laser field with different laser intensities. A distinct peak located at the energy of 2.17 eV corresponds to the pronounced intensity stripes indicated by 1 and 5 in the experimental data of Figs. 2c and 2d in the main text. Upon careful examination of the spectra, one can readily identify that the position of this peak is almost unchanged when the laser intensity undergoes variations, indicating that the pronounced peak arises from a Freeman resonance.

3. Relative phase between the transition amplitudes of the different atomic orbitals

To understand the interference patterns in the photoelectron angular distributions (PADs), we analyze the relative phase between the transition amplitudes of the $2s$ and $2p$ orbitals of HOMO in N_2 . For simplicity, we extract the terms relevant to the atomic orbitals from the transition amplitude in Eq. (2) of the main text:

$$c_a \langle \mathbf{Q}(t_0) | \mathbf{r} \cdot \mathbf{E}(t_0) | \psi_a \rangle \left[e^{i\mathbf{p} \cdot \mathbf{R}/2} + (-1)^{l_a} e^{-i\mathbf{p} \cdot \mathbf{R}/2} \right] \quad (\text{S1})$$

where $\mathbf{Q}(t_0) \equiv \mathbf{q}(t_0) + \mathbf{A}(t_0)$ denotes the initial momentum at the tunneling time t_0 . According to the saddle-point equation [14], $Q(t_0)^2 = -2I_p$ with the ionization potential I_p of an atom or a molecule. By expanding the atomic orbital ψ_a with a Gaussian basis set, we obtain the expanded expressions of Eq. (S1) for the perpendicular and parallel alignments, respectively.

Firstly, for the perpendicular alignment, Eq. (S1) can be expressed as

$$-i c_{2s} \cos[p_x R/2] e^{-Q^2/(4\zeta_{2s})} E_z Q_z \pi^{3/2} / (2\zeta_{2s}^{5/2}) \quad (\text{S2})$$

for the $2s$ atomic orbitals and

$$-i c_{2p} \sin[p_x R/2] e^{-Q^2/(4\zeta_{2p})} E_z Q_z p_x \pi^{3/2} / (2\zeta_{2p}^{5/2}) \quad (\text{S3})$$

for the $2p$ atomic orbitals. Here, we assume that the electric field of the laser field is along the z direction. Q_z denotes the photoelectron momentum at the time t_0 along the z direction and p_x denotes the final momentum of the photoelectron along the x direction. Considering that the coefficients ζ_{2s} and ζ_{2p} in the Gaussian basis are positive real numbers and the value of p_x is small and real, it can be found that the relative phase between the two equations is determined by the coefficients c_{2s} and c_{2p} . Therefore, the phase difference between the transition amplitudes of the $2s$ and $2p$ orbitals, $\arg[M(\mathbf{p})_{2s}] - \arg[M(\mathbf{p})_{2p}]$, corresponds to the relative phase between c_{2s} and c_{2p} .

Secondly, for the parallel alignment, Eq. (S1) can be written as

$$-i c_{2s} \cos[p_z R/2] e^{-Q^2/(4\zeta_{2s})} E_z \pi^{3/2} Q_z / (2\zeta_{2s}^{5/2}) \quad (\text{S4})$$

for the $2s$ atomic orbitals and

$$-i c_{2p} \sin[p_z R/2] e^{-Q^2/(4\zeta_{2p})} E_z \pi^{3/2} \left[\frac{Q_z^2}{(4\zeta_{2p}^{7/2})} - 1 / (2\zeta_{2p}^{5/2}) \right] \quad (\text{S5})$$

for the $2p$ atomic orbitals. Similarly, by comparing with the two equations, we find that the momentum Q_z along the laser polarization, which is purely imaginary according to the saddle-point equation [14], will also make effect in the relative phase. Therefore, aside from the phases of the coefficients c_{2s} and c_{2p} , an additional phase of $\pi/2$ contributes to the phase difference between the transition amplitudes of the $2s$ and $2p$ orbitals.

4. M-CQSFA-simulated PAD of a larger molecule

Here, we also simulate the PAD of a larger molecule, i.e., N_2H_2 , or Diazene. For better comparison with the PAD of the simple molecule N_2 , we consider the HOMO-2 of N_2H_2 (shown in Fig. S3(a)), which has the same σ_g symmetry as the HOMO of N_2 . Fig. S3(b) shows the simulated PAD of N_2H_2 with the M-CQSFA theory, in which a rich interference pattern can be observed. For example, there are four peculiar peaks off the white dashed curve with the momentum of $|p| = 0.5$ a.u., which are marked by four arrows in the PAD. The two peaks marked by the red arrows can be found in the PAD of two N atoms, as shown in Fig. S3(c). Their energy shift originates from the interference of the s and p atomic orbitals of the two N atoms. On the other side, the two peaks marked by the blue arrows can be observed in PAD of two H atoms in Fig. S3(d) and the energy shift is due to the two-center interference from the two s orbitals of the two H atoms [37]. The use of these peculiar interference features in the PADs will benefit the accurate reconstruction of more complicated molecular orbitals with our imaging method.

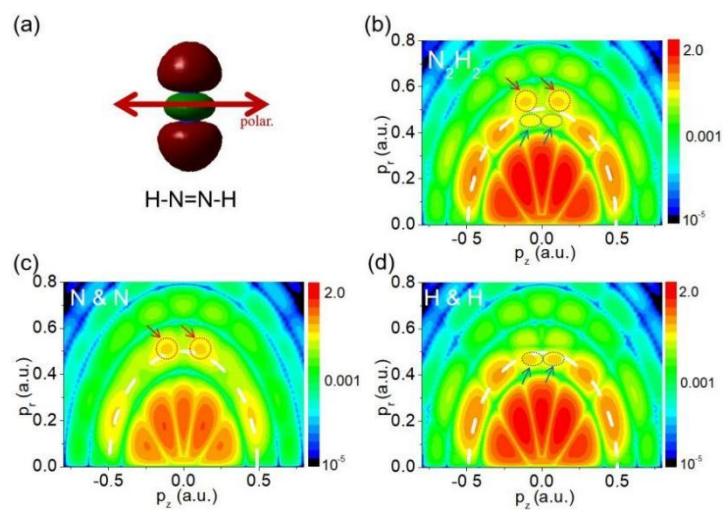


Fig. S3: (a) Schematic view of the strong-field ionization of the molecule N_2H_2 in HOMO-2 with σ_g symmetry. The laser polarization is perpendicular to the molecular axis. (b) Simulated PADs of N_2H_2 with the M-CQSFA theory, in which four peculiar peaks are marked by four arrows. (c) and (d) M-CQSFA simulated PADs from two N atoms and two H atoms, respectively.